

ChemComm

Accepted Manuscript



This is an *Accepted Manuscript*, which has been through the Royal Society of Chemistry peer review process and has been accepted for publication.

Accepted Manuscripts are published online shortly after acceptance, before technical editing, formatting and proof reading. Using this free service, authors can make their results available to the community, in citable form, before we publish the edited article. We will replace this *Accepted Manuscript* with the edited and formatted *Advance Article* as soon as it is available.

You can find more information about *Accepted Manuscripts* in the [Information for Authors](#).

Please note that technical editing may introduce minor changes to the text and/or graphics, which may alter content. The journal's standard [Terms & Conditions](#) and the [Ethical guidelines](#) still apply. In no event shall the Royal Society of Chemistry be held responsible for any errors or omissions in this *Accepted Manuscript* or any consequences arising from the use of any information it contains.



Journal Name

COMMUNICATION

Improved Pharmacokinetics of Mercaptopurine Afforded by a Thermally Robust Hemihydrate

Received 00th January 20xx,
Accepted 00th January 20xx

Kortney M. Kersten,^a Adam J. Matzger^{*a,b}

DOI: 10.1039/x0xx00000x

www.rsc.org/

Structural and thermal data were obtained for a novel hemihydrate of 6-mercaptopurine. The hemihydrate shows increased solubility and bioavailability when compared to the monohydrate form, better stability against conversion in aqueous media than the anhydrate form, and a dehydration temperature of 240 °C, the highest of any known hydrate crystal.

Solvated forms of drugs are commonly encountered during solid form discovery efforts. Hydrates, in particular, are of significance due to their impact on the properties of active pharmaceutical ingredients (APIs)¹ and the potential for them to form in vivo. Water can fill gaps in the crystal structure of a compound, as well as stabilize a solid state arrangement through hydrogen bonding with API molecules.² The presence of water in a crystal structure also affects physical properties such as the solubility and thermal stability of the compound. While not always the case,³⁻⁵ the more water that is incorporated into the solid state structure of a compound, the lower its aqueous solubility typically will be.^{1, 6} Therefore it would seem that the anhydrous form of a compound would most often be the obvious choice for commercialization. However, almost half of pharmaceuticals with a known hydrate form are used commercially as the hydrate.⁷ Indeed, solubility is not the only factor to consider.

When selecting the solid form of a pharmaceutical to develop into a dosage both stability and solubility are considered. Although solubility considerations tend to favor using anhydrous forms, the desire for stability during processing and storage may favor the development of hydrates. During processing into tablets or capsules, APIs are subjected to different humidities, pressures, and temperatures that may alter their solid form.^{1, 8} Choosing the most

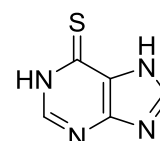


Figure 1. Structure of mercaptopurine.

soluble form of a drug may allow it to change forms once processed and could lead to non-uniformity of dosage. For example, the use of moxifloxacin hydrochloride led to inconsistent active content during administration, a problem that was overcome with use of a novel hydrate.⁹ For these reasons, determining the resistance of a compound to changes in hydration state under different temperature and water activities is just as important as solubility when considering the ideal form of a pharmaceutical.

Mercaptopurine (Figure 1), developed in the 1950s, was one of the first marketed antileukemia drugs and helped earn Elion and Hitchings the Nobel Prize in 1988.¹⁰ Though the anhydrate structure is also known, mercaptopurine is sold as the monohydrate form under the commercial name of Purinethol. Mercaptopurine acts as a purine inhibitor in the body, and has shown high activity ($IC_{50} = 0.5 \mu M$) in some cancer cell lines.¹¹ However, the commercial form is plagued by low water solubility (0.249 mg/mL at 37 °C) which may affect its bioavailability.¹² The anhydrous form is more soluble, but suffers from poor stability (vide infra). Herein, we report the crystal structure and properties of a novel hemihydrate form of mercaptopurine. The hemihydrate shows higher water solubility and bioavailability than the commercial form. Moreover, this new form has a dehydration temperature of 240 °C, which is, to our knowledge, the highest seen of any single component hydrate in the literature.¹³⁻¹⁷ This combination of solubility and stability may be useful from a pharmaceutical standpoint to increase the bioavailability of this API.

^a Department of Chemistry, University of Michigan, Ann Arbor, Michigan 48109-1055, USA. E-mail: matzger@umich.edu

^b Macromolecular Science and Engineering, University of Michigan, Ann Arbor, Michigan 48109-1055, USA

† Electronic Supplementary Information (ESI) available: Experimental and characterization. CCDC 1447142 See DOI: 10.1039/x0xx00000x

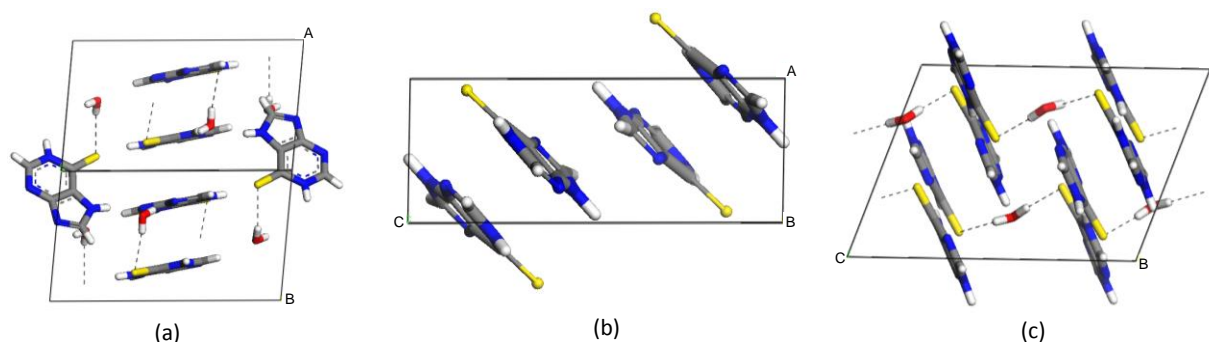


Figure 2. Crystal structures of mercaptopurine (a) monohydrate, (b) anhydrate, and (c) hemihydrate forms.

In order to access the hemihydrate form, careful consideration must be given to the solvent used and the amount of water introduced into the system. The hemihydrate crystal can be obtained by heating the commercial form in methanol (4 mg/mL) at 80 °C for 30 minutes and filtering this solution (4.5 mL) into a vial containing 0.5 mL water. When capped and allowed to sit at room temperature for two days, the hemihydrate forms as clusters of yellow needles.

Initial characterization of this novel form was performed by Raman spectroscopy as well as Powder X-ray Diffraction (PXRD). Characteristic differences are apparent among all three forms of mercaptopurine by Raman spectroscopy in the region of 350 to 750 cm^{-1} (Fig. S1 and S2 in ESI[†]). Computation of the vibrational modes of the isolated molecule assigns the observed peaks in this region to different modes of ring deformation and hydrogen wagging, expected for molecules containing purine rings.¹⁸ These differences suggest alterations in packing among the three forms that restrict the ring breathing in various ways. The PXRD patterns of the hemihydrate and anhydrate, though similar, are easily distinguishable from the monohydrate (Fig. S5 in ESI[†]). Similarities in the powder patterns between the hemihydrate and anhydrate suggest an almost isostructural relationship. However, minor differences can be seen in the 20 to 30° 2 θ range. Additional characterization such as Karl Fisher titration and elemental analysis were used to determine the purity and homogeneity of the hemihydrate crystals (See ESI for details). A single crystal of

sufficient quality was isolated for structural determination and the hemihydrate structure is shown in Figure 2 in comparison to the known forms.

Investigation of the structures (hydrogen atom positions normalized in Mercury) indicates that the water molecules are incorporated into the structure differently in the monohydrate and hemihydrate forms. In the monohydrate, one water molecule hydrogen bonds to the sulfur of one mercaptopurine molecule (2.40 Å) and an imidazole nitrogen in another (1.82 Å). Two mercaptopurine molecules and two water molecules make a rhombus-shaped complex. These units are connected together into chains by hydrogen bonding between the oxygen of the water molecules and the pyrimidine N-H (1.75 Å). These two dimensional chains are linked through the imidazole N-H hydrogen bonds to a pyrimidine nitrogen in a mercaptopurine molecule of another chain at an N-H...N angle of 109° (1.90 Å). In the hemihydrate structure, however, one water molecule asymmetrically hydrogen bonds in between the sulfur atoms of two mercaptopurine molecules (2.37 and 2.45 Å) in a zigzag manner. Two mercaptopurine molecules are then linked between both N-H(imidazole)...N(pyrimidine) sites with hydrogen bonds (1.87 and 1.88 Å). The zigzag chains are linked between N-H(pyrimidine)...N(imidazole) sites by hydrogen bonding (1.81 Å). The oxygen of the water molecule does not participate in hydrogen bonding in this structure. The sulfur-centered hydrogen bonds to water in each structure are very similar and the distances are consistent with moderate strength.¹⁹ The monohydrate structure

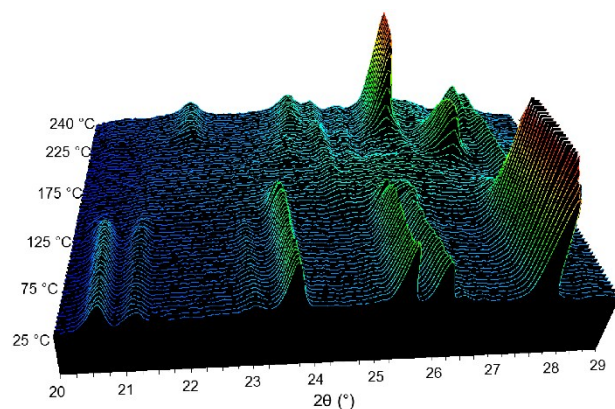


Figure 3. Variable Temperature PXRD patterns obtained from heating the monohydrate form.

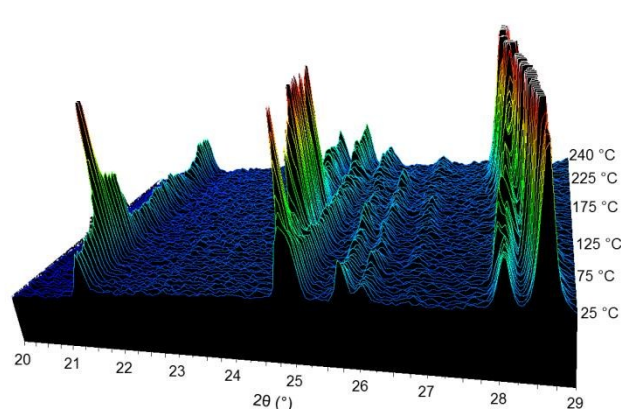


Figure 4. Variable temperature PXRD patterns obtained from heating the hemihydrate form.

overall contains more hydrogen bonding; however, the hemihydrate form shows substantially increased thermal stability (vide infra) that is not explained by the aforementioned crystal packing. Investigation also shows that the anhydrate and hemihydrate forms have very similar crystal packing, and identical hydrogen bonding graph sets, but the hemihydrate has water residing in empty pockets formed throughout the anhydrate structure, causing only minor disturbances (See Fig. S7 and S8 in ESI[†]).

DSC analysis and variable temperature PXRD were used to analyze the thermally-induced phase transitions of the compounds. The monohydrate form shows a loss of crystallinity at ~160 °C followed by a recrystallization into the anhydrate structure (Figure 3). In a sealed DSC pan, two events can be observed at ~150 °C and ~180 °C (Fig. S9 in ESI[†]). Modulated DSC shows that the event at ~150 °C is non-reversible, and corresponding that with the weight loss of 10% observed between 100-150 °C by Thermogravimetric Analysis (TGA) (Fig. S10 and S15 in ESI[†]), suggests this event is loss of water from the crystals. The event at ~180 °C, however, shows some reversible character, suggesting this is the loss of crystallinity. This matches previous literature reports.²⁰ In a DSC pan with a hole poked in the lid, allowing water vapor to escape, the two events merge into one broader endothermic event with a T_{\max} of 177 °C (Fig S7 in ESI[†]), but modulation shows equivalent non-reversible and reversible events occurring at the same temperatures as in the closed pan. The hemihydrate, however, does not show any loss of crystallinity during conversion to the anhydrate structure (Figure 4) with water loss occurring in a sharp endothermic event at ~240 °C by DSC as well as a 5% weight loss occurring between 200-250 °C by TGA (Fig. S13 and S16 in ESI[†]). Modulated DSC shows that this event is mainly non-reversible which is consistent with loss of water from the crystals (Fig S14 in ESI[†]). Additional energy is needed to remove water from the hemihydrate form, suggesting a greater stability to environmental conditions.

In order to determine the stability to hydration, aqueous slurries of the anhydrate and hemihydrate forms were monitored using a non-contact Raman probe (Fig. S3 and S4 in ESI[†]). While the anhydrate form converts to the monohydrate in approximately 2-5 hours on average, the hemihydrate is much more stable. On average, it begins converting after approximately 5 hours, but does not fully convert to the monohydrate until approximately 70 hours. Overall, this shows that the hemihydrate is significantly more stable in aqueous solutions than the anhydrate form, and while they will both transform to the monohydrate eventually, the hemihydrate form takes much longer to do so. This suggests a potential advantage in making a more bioavailable formulation with the hemihydrate (vide infra).

To determine the maximum solubility in water of all three forms of mercaptopurine, turbidity measurements were used to monitor particles in solution and determine the solubility at different temperatures. The monohydrate showed an average solubility of

Table 1. Pharmacokinetic parameters for mercaptopurine forms.

	Monohydrate	Anhydrate	Hemihydrate
T_{\max} (hr)	0.83 ± 0.29	0.83 ± 0.29	1.67 ± 0.58
C_{\max} (µg/mL)	0.23 ± 0.05	0.26 ± 0.01	0.28 ± 0.11
AUC (µg·hr/mL)	0.21 ± 0.06	0.43 ± 0.03	0.57 ± 0.12
% F	1.4	2.9	3.8
F_{rel}	1	2	2.7

T_{\max} = Time when maximum concentration reached

C_{\max} = Maximum concentration reached

AUC = Area under the curve

F = Bioavailability

F_{rel} = Relative bioavailability (% F_{form} / % $F_{\text{monohydrate}}$)

0.249 mg/mL at 37 °C, which is consistent with the literature.²⁰ The anhydrate showed an average solubility of 0.400 mg/mL at 37 °C, approximately double that of the monohydrate, which is also consistent with previous reports.^{21,22} The hemihydrate form might be expected to have a solubility in between these two, but in fact showed a solubility very similar to the anhydrate, at 0.390 mg/mL at 37 °C.

From these data, we hypothesized that the hemihydrate would show increased bioavailability over the monohydrate form and pharmacokinetic studies in rats were conducted (See ESI[†] for details). The bioavailability of the three forms was determined by comparison of suspension and intravenous administration in order to quantify the effect. As shown in Table 1, the hemihydrate did in fact show increased average pharmacokinetic parameters over the monohydrate form and also exceeded the performance of the anhydrate form. The hemihydrate is 2.7 times more bioavailable than the monohydrate form; this exceeds what is predicted solely from solubility. The hemihydrate is also twice as bioavailable as the anhydrate; increased resistance towards conversion of the hemihydrate compared to the anhydrate in aqueous solutions offers a plausible explanation. Since the T_{\max} was much higher for the hemihydrate than for the other two forms, it seems more compound was able to be absorbed overall even though over a somewhat longer time period, whereas the monohydrate and anhydrate were limited due to the solubility of the monohydrate

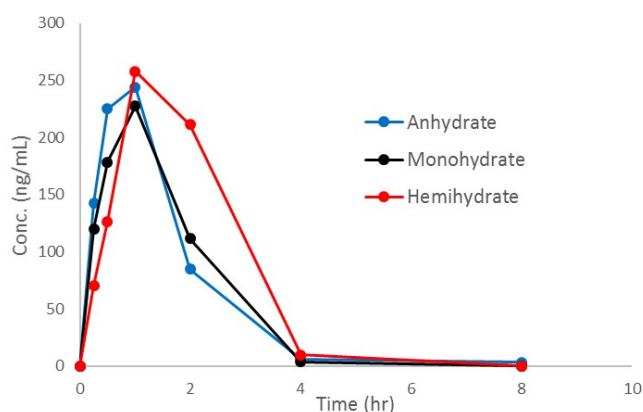


Figure 5. Pharmacokinetic profiles of the average plasma concentrations for each form. There were $n = 3$ rats in each group.

form (Figure 5) (See ESI† for details on calculations of each parameter).

In order to better understand the differences seen in bioavailability, the intrinsic dissolution rates (IDR) of the anhydrate and hemihydrate were collected using both water and the 0.5% methyl cellulose solution used for oral dosing in the pharmacokinetic studies (Fig. S17 and S18 in ESI†). (Using the rotating disk method, the IDR of the monohydrate was unable to be calculated due to an inability to firmly press tablets with either powdered or crystalline material.) In water, the average IDR of the hemihydrate is 0.327 $\mu\text{g}/\text{cm}^2\cdot\text{s}$, while the anhydrate shows an average IDR of 0.298 $\mu\text{g}/\text{cm}^2\cdot\text{s}$. In 0.5% methyl cellulose solution however, the average IDR of the hemihydrate is 0.536 $\mu\text{g}/\text{cm}^2\cdot\text{s}$ while the anhydrate is 0.660 $\mu\text{g}/\text{cm}^2\cdot\text{s}$. In water, the anhydrate form begins converting to the monohydrate at the surface of the tablet in a short amount of time, slowing its observed rate, while in the 0.5% methyl cellulose solution, conversion is suppressed and the observed rate is higher than that of the hemihydrate, which is expected based on their solubilities.

Overall, it can be seen that the newly discovered hemihydrate form of mercaptopurine shows many improved features in comparison to the known monohydrate and anhydrate forms. Not only does the hemihydrate have higher thermal stability towards dehydration than the monohydrate form, it is, to our knowledge, the highest dehydration temperature for any single component organic molecule in literature.¹³⁻¹⁷ Also, the hemihydrate form showed better stability to aqueous conversion than the anhydrate form. Finally, the hemihydrate has double the water solubility as well as almost three times the *in vivo* bioavailability of the commercially used form. The mercaptopurine hemihydrate crystal form shows remarkable properties and could have an impact on the commercial market for mercaptopurine as a pharmaceutical.

This work was supported by the National Institute of Health Grant Number RO1 GM106180. We thank Dr. Jeff Kampf for single-crystal X-ray analysis and funding from NSF Grant CHE-0840456 for the Rigaku AFC10K Saturn 994+ CCD-based X-ray diffractometer.

Notes and references

- 1 H. G. Brittain, *Polymorphism in Pharmaceutical Solids*, M. Dekker, New York, 1999.
- 2 S. R. Byrn, R. R. Pfeiffer and J. G. Stowell, *Solid-State Chemistry of Drugs*, SSCI, Inc., West Lafayette, Ind., 1999.
- 3 P. V. Allen, P. D. Rahn, A. C. Sarapu and A. J. Vanderwielen, *J. Pharm. Sci.*, 1978, **67**, 1087.
- 4 T.-C. Hu, S.-L. Wang, T.-F. Chen and S.-Y. Lin, *J. Pharm. Sci.*, 2002, **91**, 1351.
- 5 M. Shibata, H. Kokubo, K. Morimoto, K. Morisaka, T. Ishida and M. Inoue, *J. Pharm. Sci.*, 1983, **72**, 1436.

- 6 M. Pudipeddi and A. T. M. Serajuddin, *J. Pharm. Sci.*, 2005, **94**, 929.
- 7 U. J. Griesser, in *Polymorphism in the Pharmaceutical Industry*, ed. R. Hilfiker, Wiley-VCH, Weinheim, Germany, 2006, pp. 211-233.
- 8 D. Giron, C. Goldbronn, M. Mutz, S. Pfeffer, P. Piechon and P. Schwab, *J. Therm. Anal. Calorim.*, 2002, **68**, 453.
- 9 CA 2192418.
- 10 G. B. Elion, E. Burgi and G. H. Hitchings, *JACS*, 1952, **74**, 411.
- 11 T. Dervieux, J. G. Blanco, E. Y. Krynetski, E. F. Vanin, M. F. Roussel and M. V. Relling, *Cancer Research*, 2001, **61**, 5810.
- 12 L.-L. Xu, J.-M. Chen, Y. Yan and T.-B. Lu, *Cryst. Growth Des.*, 2012, **12**, 6004.
- 13 H. D. Clarke, K. K. Arora, H. Bass, P. Kavuru, T. T. Ong, T. Pujari, L. Wojtas and M. J. Zaworotko, *Cryst. Growth Des.*, 2010, **10**, 2152.
- 14 M. Karanam and A. R. Choudhury, *Cryst. Growth Des.*, 2013, **13**, 1626.
- 15 N. Mahé, B. Nicolai, M. Barrio, M.-A. Perrin, B. Do, J.-L. Tamarit, R. Céolin and I. B. Rietveld, *Cryst. Growth Des.*, 2013, **13**, 3028.
- 16 T. N. P. Nguyen and K.-J. Kim, *Ind. Eng. Chem. Res.*, 2010, **49**, 4842.
- 17 N. Variankaval, C. Lee, J. Xu, R. Calabria, N. Tsou and R. Ball, *Org. Process Res. Dev.*, 2007, **11**, 229.
- 18 J. B. Lambert, *Organic Structural Spectroscopy*, Prentice Hall, Upper Saddle River, N.J., 1998.
- 19 F. H. Allen, C. M. Bird, R. S. Rowland and P. R. Raithby, *Acta Crystallogr. Sect. B: Struct. Sci.*, 1997, **53**, 680.
- 20 M. L. Huang and S. Niazi, *J. Pharm. Sci.*, 1977, **66**, 608.
- 21 H. Nakamachi, Y. Wada, I. Aoki, Y. Kodama and K. Kuroda, *Chem. Pharm. Bull.*, 1981, **29**, 2956.
- 22 S. Niazi, *J. Pharm. Sci.*, 1978, **67**, 488.